

Tribological Property of Selective Laser Melting–Processed 316L Stainless Steel against Filled PEEK under Water Lubrication

Yinshui Liu, Xiaomin Zhai, Yipan Deng & Defa Wu

To cite this article: Yinshui Liu, Xiaomin Zhai, Yipan Deng & Defa Wu (2019): Tribological Property of Selective Laser Melting–Processed 316L Stainless Steel against Filled PEEK under Water Lubrication, Tribology Transactions, DOI: [10.1080/10402004.2019.1635671](https://doi.org/10.1080/10402004.2019.1635671)

To link to this article: <https://doi.org/10.1080/10402004.2019.1635671>



Accepted author version posted online: 09 Jul 2019.
Published online: 13 Aug 2019.



[Submit your article to this journal](#) 



Article views: 20



[View Crossmark data](#) 



Tribological Property of Selective Laser Melting–Processed 316L Stainless Steel against Filled PEEK under Water Lubrication

Yinshui Liu, Xiaomin Zhai, Yipan Deng, and Defa Wu

State Key laboratory Digital Manufacturing Equipment and Technology, Huazhong University of Science and Technology, Wuhan, P. R. China

ABSTRACT

As a 3D printing technology, selective laser melting has remarkable advantages such as high processing flexibility, high material utilization, and short production cycle. The applications of selective laser melting technology in industry have become quite extensive. There are many tribological studies on selective laser melting materials, but few based on water lubrication (Zhu, et al., *Journal of Zhejiang University-Science A*, **19**(2), pp 95–110). In this article, the tribological properties of 316L stainless steel processed by selective laser melting and traditional methods have been studied under water lubrication. Polyether ether ketone (PEEK) filled with carbon fiber (CF)/polytetrafluoroethylene (PTFE)/graphite was selected as the counterpart. 316L stainless steel and PEEK are a tribopair commonly used in water hydraulics. This study is of great significance to the application of selective laser melting material of tribopairs in water hydraulics. Friction and wear tests were carried out on a pin-on-disc contact test apparatus under different operating conditions. The friction coefficient, specific wear coefficient, scanning electron microscopy (SEM) of the worn surface, and energy-dispersive spectroscopy (EDS) of the surface adhesions of the three tribopairs were measured and compared. The results revealed that the friction coefficient of the selective laser melting (SLM) 316L stainless steel was significantly higher than that of traditionally processed (TP) 316L stainless steel, which might be caused by the pores on the surface of SLM 316L stainless steel. Adhesion and cutting on the surface of SLM 316L stainless steel were also more serious, resulting in a higher specific wear coefficient of its counterpart PEEK composite compared to PEEK composite against TP 316L stainless steel.

ARTICLE HISTORY

Received 27 January 2019
Accepted 19 June 2019

KEYWORDS

Water lubrication; selective laser melting; corrosion-resistant alloy; friction and wear

Introduction

In recent years, water hydraulics technology has become a hot research field due to its advantages such as environmental friendliness, quick response, nonflammability, and cleanliness. However, great challenges such as tribopair material selection can be brought about simultaneously due to the low viscosity, high vapor pressure, and corrosion in water (Yang, et al. (1)). With the development of material science, engineering materials with good corrosion resistance such as stainless steels, engineering plastics, and ceramics have been applied to water hydraulics components. Furthermore, stainless steels make up a high proportion of materials used in water. The application of 3D printed stainless steel to water hydraulics technology has rarely been reported.

3D printing metal plays an increasingly important role in the development of the manufacturing industry. It has been applied in many fields such as medicine, food, aviation, and so on in the United States, China, Sweden, and Germany (Godoi, et al. (2); Goole and Amighi (3); Ahmad, et al. (4)). Selective laser melting (SLM) is based on the incremental manufacturing method of layer-by-layer cladding, which can be used to process complicated parts. SLM has been widely

used in the manufacture of nonferrous metals that have potential applications in the fields of medicine and automobile and aircraft manufacturing, such as aluminum, titanium, and nickel alloys (Attar, et al. (5); Amato, et al. (6); Zhang, et al. (7)).

Antony and Murugan (8) found that SLM parts have better corrosion resistance than traditional ones meeting the requirements of water hydraulics for corrosion resistance of materials. However, the processing conditions of SLM have a great influence on the temperature distribution, transient stress, residual stress, and deformation of the material. Dai and Shaw (9) investigated the effects of laser processing conditions on multimaterial. The results indicated that the temperature distribution, transient stress, residual stress, and distortion of a multimaterial component are related to the laser processing conditions as well as the material properties, especially the thermal conductivity and coefficient of thermal expansion. Li, et al. (10) found that excessively high or low laser power causes cracks; thus, by choosing an appropriate laser power, crack-free scan tracks could be produced with no crystallization. It is known that proper process parameters can greatly improve material performance.

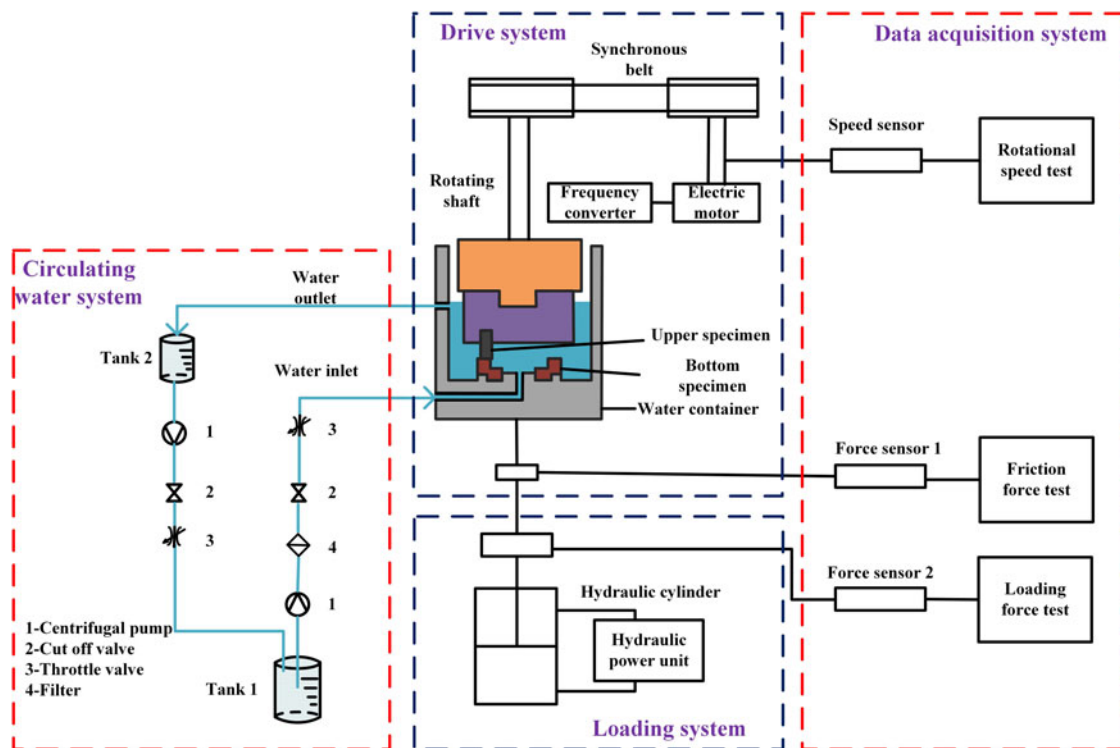


Figure 1. Schematic diagram of the experimental rig.

In recent years, researchers in the field of tribology have focused on 3D printing materials. These studies mainly focus on the tribological properties of 3D printing materials under dry friction (Zhu, et al. (11)). Kumar and Kruth (12) studied the tribological properties of SLM materials under fretting dry wear test. The results showed that the wear resistance of SLM materials is better than that of traditionally processed (TP) materials. It was found that by careful optimization of SLM parameters, better wear resistance of fully dense materials could be obtained. Sun, et al. (13) found that the specific wear coefficient of SLM steel depends on the volume percentage porosity in the steel and it is possible to achieve wear resistance similar to that of standard bulk 316L steel by obtaining full density. However, there are few tribological studies on SLM materials under lubricating conditions. By selecting the appropriate process parameters, Zhu, et al. (14) found that an SLM-processed sample had slightly lower friction and wear than a TP sample when in contact with brass under oil lubrication. However, when paired with harder materials, the difference in friction and wear between SLM process and TP was large. The internal porosity of SLM parts was caused by a balling phenomenon. Balling appears when the molten material does not wet the underlying substrate as a result of surface tension (Zhu, et al. (15)). However, there are fewer studies on SLM materials as tribopairs under the condition of water lubrication than oil lubrication. Relevant work will be carried out in this article that is of great significance for the application of SLM materials in water hydraulics.

Polyether ether ketone (PEEK) was selected as the counterpart material in this study. Many studies have shown that fiber-reinforced PEEK exhibits good tribological properties under dry friction and lubrication conditions (Davim, et al. (16); Davim and Cardoso (17)). In recent years, PEEK has been found to show great application potential in water

hydraulics components such as water plunger pumps. The tribological behaviors of filled PEEK under water lubrication have attracted increasing attention in recent years. Davim, et al. (18) studied the effect of carbon fiber reinforcement on the friction behavior of PEEK in a water-lubricated environment. It was found that the contact stress led to an almost negligible effect on the friction behavior of PEEK-CF30 and natural PEEK, and unidirectional sliding velocity had a greater influence on natural PEEK than on PEEK-CF30. Jiao, et al. (19) found that the appropriate increase in carbon fiber (CF) content can enable PEEK to obtain better antifriction performance under water lubrication. Zhang, et al. (20) compared the tribological behavior of 30 vol% CF-reinforced PEEK and PEEK filled with 30 vol% CF/polytetrafluoroethylene (PTFE)/graphite when sliding against AISI630 steel under seawater lubrication and found that the PEEK filled with 30 vol% CF/PTFE/graphite exhibited better friction and wear properties. However, there is little research focus on the tribological behaviors of filled PEEK against SLM processed parts under water lubrication in the published literature.

In this article, the tribological properties of 316L stainless steel processed by SLM and traditional cold drawing processes were studied and compared under water lubrication. PEEK filled with 30 vol% CF/PTFE/graphite (10% each) was selected as the counterpart due to its increasingly broad applications in water hydraulics components.

Experimental methods

Test equipment

The tribological behaviors of SLM 316L and TP 316L stainless steel against filled PEEK under water lubrication were

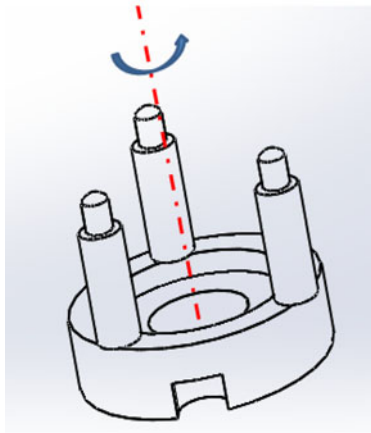


Figure 2. Friction form.

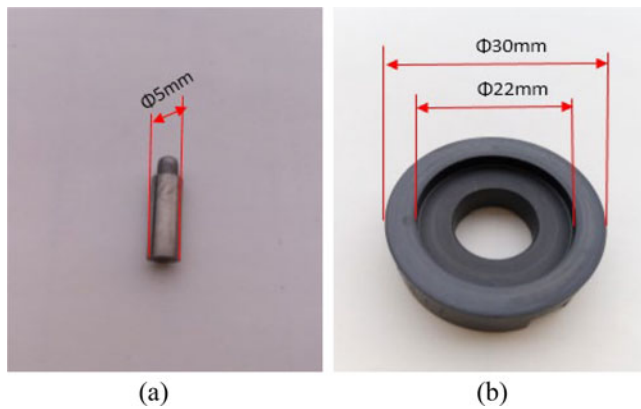


Figure 3. Schematic dimensions of the (a) upper specimens (316L stainless steel) and (b) lower specimens (PEEK).

investigated using an MM-U10A pin-on-disc rig. Figure 1 shows a schematic diagram of the test rig, which consists of a loading system, a drive system, a data acquisition system, and a circulating water system. The bottom specimen is installed in the water container, and the upper specimen rotates with the rotating shaft. Figure 2 shows the friction form. The loading system consists of two main parts: a hydraulic power unit and a hydraulic cylinder. The load is controlled by adjusting the outlet pressure of the hydraulic output unit and can be measured by the force sensor, and the rotational speed can be adjusted by the drive system and measured by the speed sensor. During the tests, water is pumped into the water container at a pressure of about 1 bar and flow rate of 0.6–0.8 L/min.

Sample preparation

Three metal pins of the same material were used as the upper specimens, and PEEK filled with 30 vol% CF/PTFE/graphite was used as the lower specimens. A schematic of the dimensions of the upper and lower specimens is shown in Fig. 3. The lower samples were produced using the traditional process. The upper samples were made of 316L stainless steel produced using SLM and the traditional process, respectively. SLM was performed using a Concept Laser M2 cusing metal laser 3D printer composed of a 180-W fiber laser, an argon gas protection system, and a process control

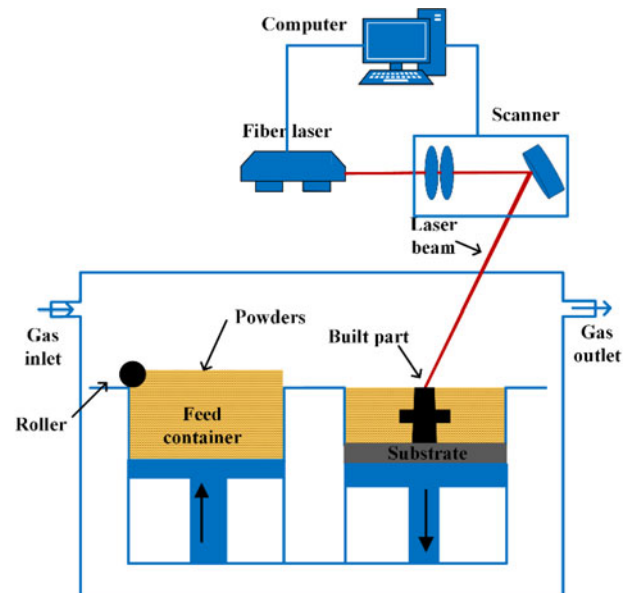


Figure 4. Schematic of the SLM system.

system. A schematic of the SLM system is shown in Fig. 4. Relevant SLM process parameters are listed in Table 1, where the point distance represents the distance between the adjacent laser points. These parameters are commonly used for processing 316L stainless steel with excellent properties. 316L stainless steel powders are spherical in shape, as shown in Fig. 5. Powders with a size range of 15–45 μm were supplied by Concept Laser. The material composition of SLM 316L stainless steel is shown in Table 2. Post-heat treatment was performed to eliminate internal stress, as shown in Fig. 6.

Before the test, the PEEK composite was immersed in tap water for 7 days until no longer absorbed water (Li, et al. (21)). Before testing, the contact surfaces of the upper and lower specimens were polished with abrasive papers (p1000, p2500, p5000, sequentially). To prevent the pins' sharp edges from cutting the PEEK specimens, the edges of the pins were rounded. A comprehensive measurement system for surface profile measurement was used to measure the surface roughness of the upper and lower specimens after polishing. Each specimen was measured three times along the circumferential and radial directions and the average value was obtained. The measured values of three pins of SLM 316L stainless steel were $R_a = 0.0092$, $R_a = 0.0118$, $R_a = 0.0111$ μm , respectively. The measured values of three pins of TP 316L stainless steel were $R_a = 0.0076$, $R_a = 0.0085$, $R_a = 0.0083$ μm , respectively. By comparing SLM 316L stainless steel with TP 316L stainless steel, it was found that the former has a higher surface roughness than the latter, which might be caused by the pores on the surface of SLM 316L stainless steel. The average roughness of PEEK composite was 0.06 μm . After polishing, the specimen must be treated strictly according to the steps of cleaning for 5 min, blowing by a blower for 3 min, drying in a drying cabinet for 5 min, and weighing. Weighing must be carried out according to the above steps before and after the test.

The tribological properties of the materials were judged by three indexes: the friction coefficient, the specific wear

coefficient, and the worn surface morphology. The friction and wear test lasted 150 min. The friction coefficient was recorded every 1 s. Finally, the curves of the friction coefficient over 150 min for all three materials were compared. The mass of the specimens was measured separately three times before and after the test by an analytical balance with a resolution of 0.01 mg. The specific wear coefficient was calculated based on the following formula:

$$W = \frac{\Delta m}{\rho \cdot L \cdot Q},$$

where W is the specific wear coefficient, Δm is the wear mass, ρ is the density, L is the friction distance, and Q is the load.

Materials and specimens

The physical and mechanical properties of PEEK composite provided by the manufacturer are listed in Table 3. The hardness of the SLM 316L stainless steel and TP 316L stainless steel are listed in Table 4 as measured on a Vickers hardness tester three times at three different points to obtain the average hardness. Other parameters were provided by the manufacturers. The SLM 316L stainless steel has a lower hardness than TP 316L. Zhu, et al. (14) optimized the process parameters and found that there were still some obvious pore defects in SLM 316L stainless steel. The surface micropores of SLM 316L stainless steel were observed by scanning electron microscopy (see Fig. 7). The pores in Fig. 7 have an irregular shape with a maximum of approximately 10 μm .

Operating conditions

In a typical water piston pump, the product of load and sliding velocity of the tribopair is 0–3.67 MPa·m/s (Liu, et al.

Table 1. SLM processing parameters.

Spot size	Laser power	Scan speed	Layer thickness	Point distance
70 μm	180 W	600 mm/s	30 μm	60 μm

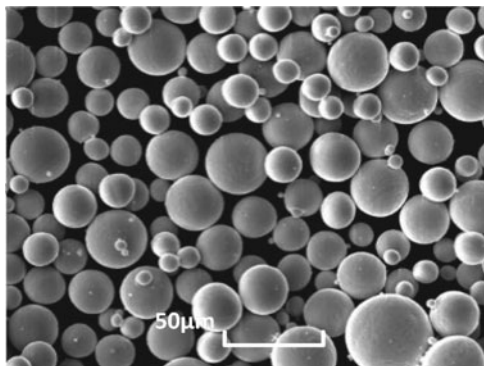


Figure 5. SLM 316L stainless steel powder image.

Table 2. Chemical composition of SLM 316L.

Chemical composition (wt%)	Fe	Cr	Ni	Mo	Mn	Si	P	C	S	Cs
SLM 316L	Balance	16.5–18.5	10.0–13.0	2.0–2.5	0–2.0	0–1.0	0–0.045	0–0.030	0–0.030	0–0.03

(22)). Therefore, the loads adopted in the experiments were 50 and 100 N (corresponding stress: 0.85 and 1.7 MPa). The rotation speeds were 500 and 1,000 rpm, and the corresponding sliding velocities were 0.68 and 1.36 m/s, respectively. In addition, each test under one specific condition with a new set of friction specimens was repeated three times, and the average values of three repeated tests are presented.

Friction and wear results

Friction coefficient

Figure 8 shows the change in friction coefficient with time from three sets of repeated experimental data. In order to precisely evaluate the friction coefficient, we calculated the average value and standard deviation. The mean of the average friction coefficient and the mean of the standard deviation of three sets of repeated tests were calculated after 30 min, because the initial plane had little effect on the friction process after this time. For each single test an average friction coefficient and a standard deviation of friction were determined. Figure 9a shows the mean of the average friction coefficient values and the standard deviation. Figure 9b shows the mean of the standard deviation values and the standard deviation of standard deviation values. According to the statistical theory, a higher standard deviation indicates that the friction coefficient fluctuates more drastically with time. Figure 9b shows that the standard deviation of SLM 316L stainless steel is always high under different working conditions, indicating that the friction process is unstable. The unstable friction process might be caused by the pores

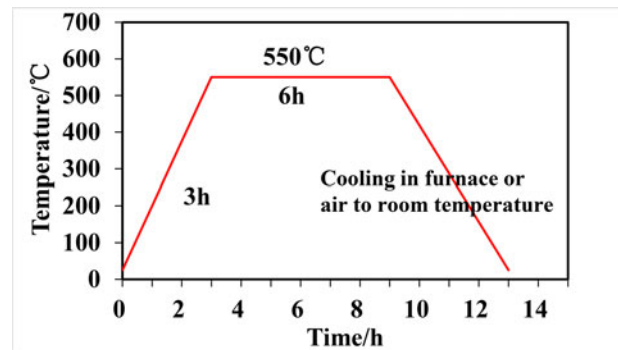


Figure 6. Post-heat treatment process of SLM 316L parts.

Table 3. Properties of PEEK composite.

Properties	Unit	Test method		Value
		DIN	ASTM	
Density	g/cm^3	53479		1.48
Tensile strength at break	MPa	53455		118
Glass transition	$^{\circ}\text{C}$	5336		143
Water absorption (by immersion) at 23 $^{\circ}\text{C}$	%	53495		0.1
Crystalline melting point	$^{\circ}\text{C}$	53736		334
Heat distortion temperature	$^{\circ}\text{C}$	ISO 75		277

on the surface of SLM stainless steel. As can be observed from Fig. 9a, with an increase in sliding speed, the friction coefficients of the two tribopairs significantly decreased because a hydrodynamic lubrication film was more easily formed when sliding at a high speed (Dong, et al. (23)). The friction coefficients of SLM 316L stainless steel under different operating conditions were significantly higher than that

of TP 316L stainless steel, which might be caused by the pores on the surface of SLM 316L stainless steel.

Table 4. Hardness of SLM 316L and TP 316L.

Material	SLM 316L	TP 316L
Vickers hardness (MPa)	206	304

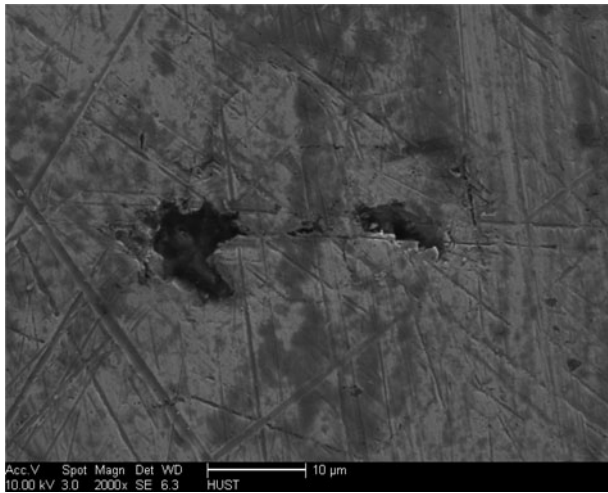


Figure 7. SEM of pores in SLM 316L stainless steel sample.

Specific wear coefficient

Figure 10 shows the specific wear coefficient of SLM 316L and TP 316L stainless steel under water lubrication at different operating conditions. In some conditions, the weights of the two kinds of stainless steel were significantly increased after the test, which is the result of some PEEK composite material being transferred onto its counterpart SLM 316L and TP 316L stainless steel. The specific wear coefficient is a common reflection of wear and material transfer in this test. From Fig. 10, the increased mass caused by the material transfer had significant effects on the specific wear coefficient of SLM 316L and TP 316L stainless steel. Under three operating conditions (50 N and 500 rpm, 100 N and 500 rpm, 100 N and 1,000 rpm), the mass of TP 316L increased after the test. Under these conditions, material transfer was the main reason for the mass change, resulting in increased mass after the experiment. The material transfer phenomenon of SLM 316L stainless steel is obviously more serious at 50 N. From the previous section, we know that the average value and standard deviation of SLM 316L friction coefficient are large at 50 N and the friction process is very unstable, which is related to a large amount of material transfer. At 100 N, the wear of SLM 316L is more serious than the material transfer, resulting in positive specific wear

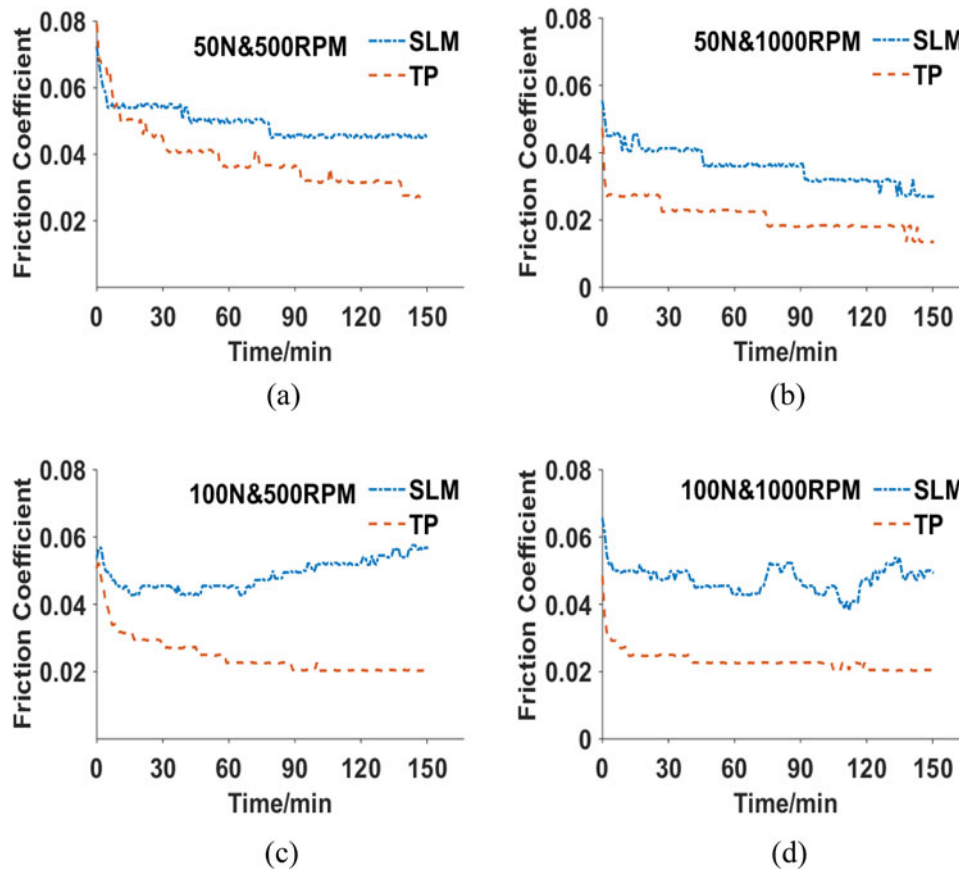
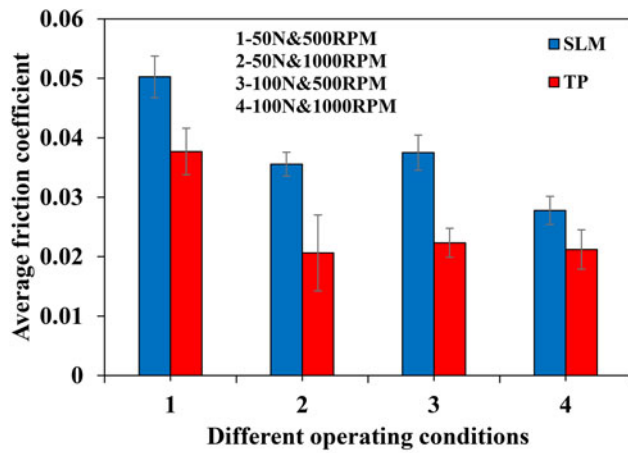
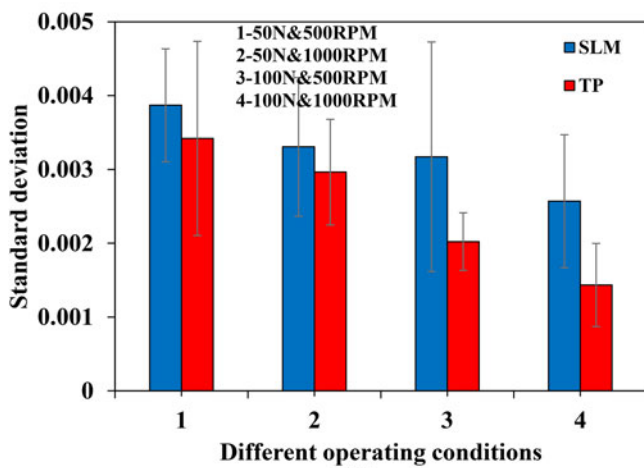


Figure 8. Friction coefficients under different conditions: (a) load: 50 N, speed: 500 rpm; (b) load: 50 N, speed: 1,000 rpm; (c) load: 100 N, speed: 500 rpm; (d) load: 100 N, speed: 1,000 rpm.



(a)



(b)

Figure 9. Mean of (a) average friction coefficient values and (b) standard deviation values under different operating conditions.

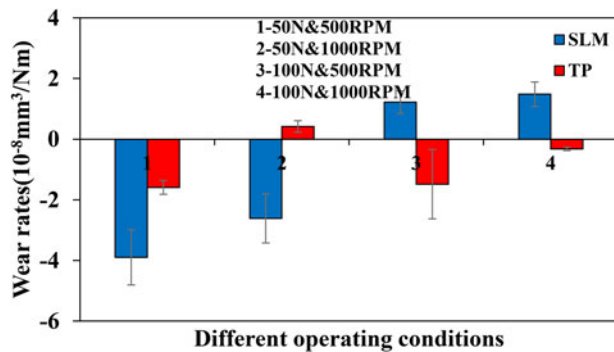


Figure 10. Specific wear coefficient of SLM 316L and TP 316L stainless steel under different operating conditions.

coefficient. Under most operating conditions, SLM 316L stainless steel always had a larger mass change before and after the experiment than TP 316L stainless steel.

Figure 11 shows the specific wear coefficient of PEEK composite under water lubrication at different operating conditions. As shown in the figure, the specific wear coefficient of PEEK composite decreased significantly with an increase in speed, which is consistent with the view that hydrodynamic lubrication is better at high speed. Compared to PEEK composite against TP 316L stainless steel, PEEK

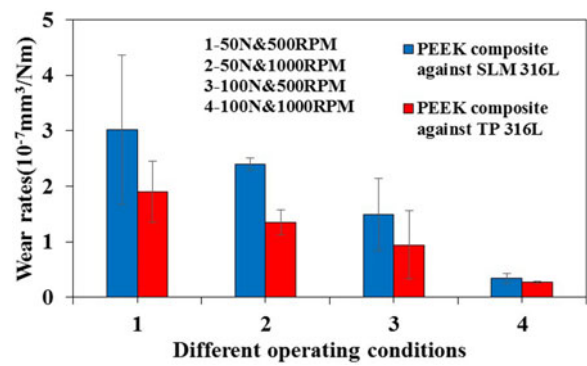


Figure 11. Specific wear coefficient of PEEK composite against SLM 316L and TP 316L stainless steel under different operating conditions.

composite against SLM 316L stainless steel was found to have a higher specific wear coefficient under all operating conditions. As can be seen from Fig. 10, SLM 316L stainless steel paired with PEEK composite had more severe material transfer at 50 N and wear at 100 N, which resulted in greater mass loss of PEEK composite. The specific wear coefficient of two PEEK composite samples was minimal at 100 N and 1,000 rpm. This might be caused by the stable friction process under this condition, which can also be observed from Fig. 9.

Scanning electron microscopy and energy-dispersive spectroscopy

In order to explain the wear mechanism of two tribopairs under water lubrication, scanning electron microscopy (SEM) was used to observe the surface morphology before and after wear. Figure 12 shows the surface morphology of the specimens before and after the test at 50 N and 1,000 rpm. As shown in Fig. 12, the surfaces of the two stainless steels present clear cutting marks and adhesion. The adhesion on the surface of SLM 316L stainless steel is more serious, which is consistent with the negative specific wear coefficient of SLM 316L stainless steel shown in Fig. 10. The surfaces of PEEK composite present gullies and material peeling. Figure 13 shows a comparison of the composition of the adhered transfer and bare areas on the surfaces of two stainless steels analyzed by energy-dispersive spectroscopy (EDS). Point 1 comes from the adhered transfer on the surface of the stainless steel and point 2 from the bare area. According to the comparison of the main chemical components of the two points, point 1 has a significantly higher peak of carbon relative to point 2, indicating that the adhered transfer came from the counterpart PEEK composite.

According to analysis of SEM and EDS, the main wear mechanisms of the two tribopairs are adhesive wear and abrasive wear under water lubrication. The adhesion of SLM 316L stainless steel is more serious at 50 N, which leads to a higher friction coefficient and increased mass after the test.

Discussion

From the analysis of the friction coefficient, specific wear coefficient, and SEM/EDS, the main wear mechanisms of

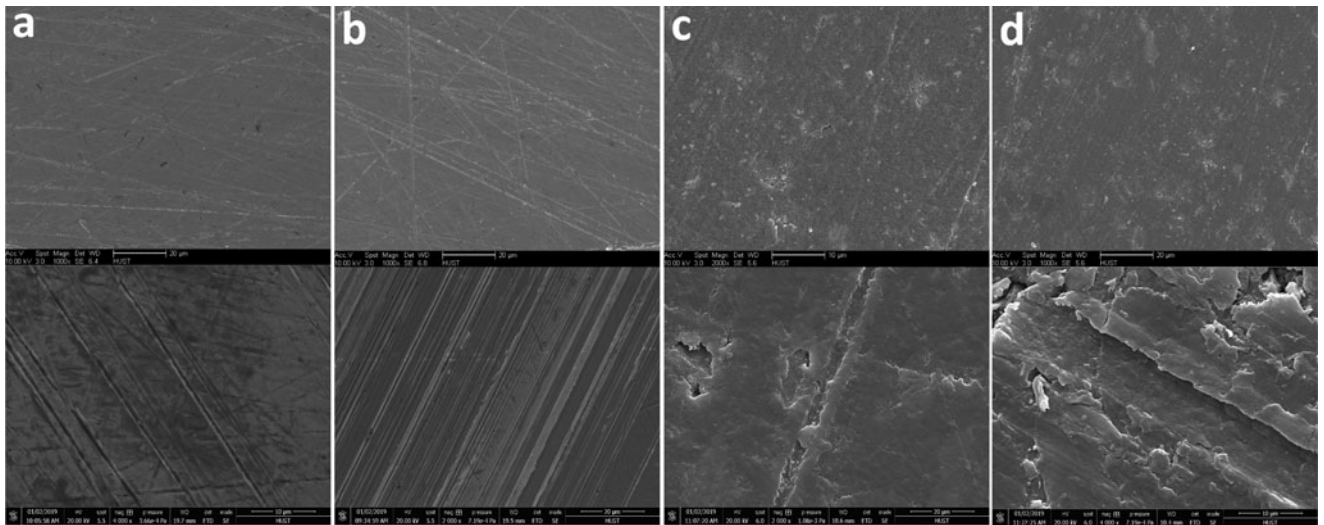


Figure 12. Surface morphology before and after wear at 50 N and 1,000 rpm: (a) SLM 316L; (b) TP 316L; (c) PEEK composite against SLM 316L; and (d) PEEK composite against TP 316L.

the two tribopairs are adhesive wear and abrasive wear, and the specific wear coefficient is the comprehensive embodiment of these two wear mechanisms. From Figs. 9a and 11, the friction coefficient and specific wear coefficient of PEEK composite decreased obviously with an increase in sliding speed. As can be seen from Fig. 9b, the standard deviation of the friction coefficient becomes increasingly smaller with an increase in sliding speed, indicating that the friction process becomes increasingly stable. This is because the hydrodynamic pressure increases with increasing sliding speed (Wu, et al. (24)). It can also be seen that in any condition, the friction coefficient of SLM material is significantly higher than that of TP material, the reason for which can be determined from Figs. 10 and 11. It can be seen from Fig. 10 that SLM materials always have greater mass changes before and after the experiment than TP materials. A negative specific wear coefficient indicates material transfer. The specific wear coefficient is jointly determined by material transfer and wear. It can be seen from Fig. 10 that the material transfer and wear of SLM materials are more serious than those of TP materials.

The higher friction coefficient and higher specific wear coefficient of PEEK composite indicate that the tribological properties of SLM materials are not as good as those of TP materials. The main reason is the porosity of SLM materials. The porosity of the SLM surface results in high roughness. At 50 N, the contact area is small and the bonding points are more easily formed on the rough surface. Therefore, adhesive wear is more likely to occur on the rough surface (Davim and Marques (25)). Because the pores of SLM material exist in the whole bare area, the pores on the surface always exist, making the surface a poor friction environment with repeated adhesion. This unstable friction environment results in a high friction coefficient of SLM stainless steel and high specific wear coefficient of PEEK composite. At 100 N, the specific wear coefficient of SLM material is positive and abrasive wear mainly occurs. The abrasive wear of TP is not obvious because the hardness of TP material is higher and the wear is difficult to determine

from the specific wear coefficient. As can be seen from Fig. 11, although the hardness of SLM material is lower than that of TP material, the specific wear coefficient of PEEK composite corresponding to SLM material is still higher than that corresponding to TP material at 100 N. This is due to the rough surface of the SLM material, which results in greater wear of PEEK composite.

It has been found that surface porosity has a good effect on the lubrication of materials. However, a literature review shows that the effect of pores on lubrication is related to the size and density of pores (Zhu, et al. (26)). The effect of pores on the friction properties of materials is not always good, and the optimal pore characteristics should be determined through screening. SLM materials in this study were processed with a set of conventional process parameters, and the process parameters were not optimized. Therefore, it is understandable that the internal pores of SLM specimens had no positive effect on lubrication in this study. In addition, the traditional process of TP materials used in this study was a cold drawing process, which is different from that used in other literature and may also be a factor in the different results.

Conclusions

The tribological behavior of SLM 316L stainless steel and TP 316L stainless steel against PEEK filled with CF/PTFE/graphite under water lubrication was studied. The following conclusions can be drawn:

1. The higher friction coefficient and higher specific wear coefficient of PEEK indicate that the tribological properties of SLM 316L stainless steel are worse than those of TP 316L stainless steel, which is mainly caused by the pores inside SLM material.
2. The main wear mechanisms of the two tribopairs were adhesive wear and abrasive wear. SLM stainless steel is

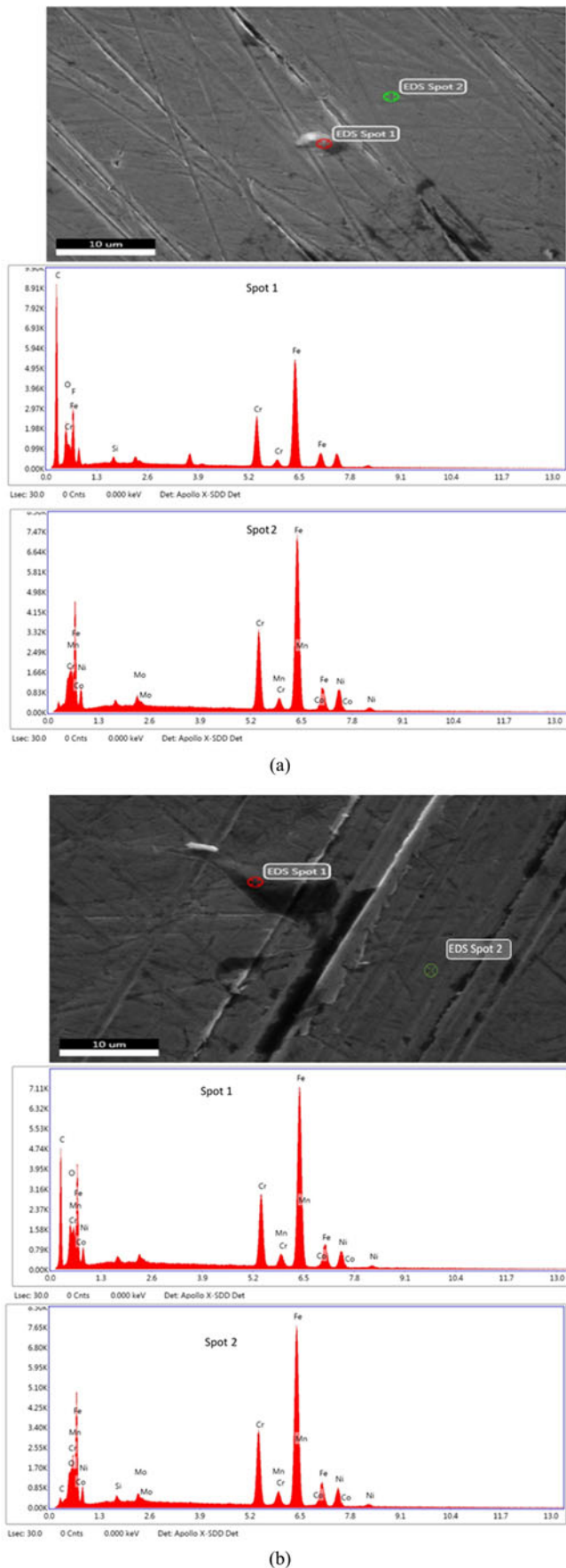


Figure 13. Comparison of the composition of adhered transfer and bare areas on the surface of two stainless steels at 50 N and 1,000 rpm: (a) SLM 316L and (b) TP 316L.

more prone to adhesive wear at low loads and abrasive wear at high loads.

- The results showed that the use of SLM 316L stainless steel as friction material under water lubrication is not advantageous. The rough surface caused by the porosity of SLM 316L stainless steel has a great impact on its tribological properties under water lubrication. SLM specimens processed with conventional process parameters are not suitable for friction materials under water lubrication. It may be possible to make up this defect by selecting better process parameters, but whether it can surpass the TP sample remains to be proved.

Acknowledgements

We are grateful to the Huazhong University of Science and Technology Test Centre for offering necessary assistance.

Funding

This article was supported by the program for National Key Research & Development Program of China (Nos. 2016YFC0300600 and 2016YFC0304800) and the National Natural Science Foundations of China (Nos. 51575200 and 51879114).

References

- Yang, H. Y., Zhou, H., and Lu, Y. X. (2000), "Research Status and Development Trend of Water Hydraulic Technology," *Chinese Journal of Mechanical Engineering*, **11**(12), pp 1430–1433.
- Godoi, F. C., Prakash, S., and Bhandari, B. R. (2016), "3D Printing Technologies Applied for Food Design: Status and Prospects," *Journal of Food Engineering*, **179**, pp 44–54.
- Goole, J. and Amighi, K. (2016), "3D Printing in Pharmaceuticals: A New Tool for Designing Customized Drug Delivery Systems," *International Journal of Pharmaceutics*, **499**(1), pp 376–394.
- Ahmad, A., Darmoul, S., Ameen, W., Abidi, M. H., and Al-Ahmari, A. M. (2015), "Rapid Prototyping for Assembly Training and Validation," *IFAC-PapersOnLine*, **48**(3), pp 412–417.
- Attar, H., Calin, M., Zhang, L. C., Scudino, S., and Eckert, J. (2014), "Manufacture by Selective Laser Melting and Mechanical Behavior of Commercially Pure Titanium," *Materials Science and Engineering: A*, **593**, pp 170–177.
- Amato, K. N., Gaytan, S. M., Murr, L. E., Martinez, E., Shindo, P. W., Hernandez, J., Collins, S., and Medina, F. (2012), "Microstructures and Mechanical Behavior of Inconel 718 Fabricated by Selective Laser Melting," *Acta Materialia*, **60**(5), pp 2229–2239.
- Zhang, L. C., Klemm, D., Eckert, J., Hao, Y. L., and Sercombe, T. B. (2011), "Manufacture by Selective Laser Melting and Mechanical Behavior of a Biomedical Ti-24Nb-4Zr-8Sn Alloy," *Scripta Materialia*, **65**(1), pp 21–24.
- Antony, K. and Murugan, S. P. (2015), "A Comparison of Corrosion Resistance of Stainless Steel Fabricated with Selective Laser Melting and Conventional Processing," *International Journal of ChemTech Research*, **7**, pp 2632–2635.
- Dai, K. and Shaw, L. (2001), "Thermal and Stress Modeling of Multi-Material Laser Processing," *Acta Materialia*, **49**(20), pp 4171–4181.
- Li, X. P., Kang, C. W., Huang, H., Zhang, L. C., and Sercombe, T. B. (2014), "Selective Laser Melting of an $\text{Al}_{86}\text{Ni}_6\text{Y}_{4.5}\text{Co}_2\text{La}_{1.5}$ Metallic Glass: Processing, Microstructure Evolution and

- Mechanical Properties,” *Materials Science and Engineering: A*, **606**, pp 370–379.
- (11) Zhu, Y., Zou, J., and Yang, H. Y. (2018), “Wear Performance of Metal Parts Fabricated by Selective Laser Melting: A Literature Review,” *Journal of Zhejiang University-Science A*, **19**(2), pp 95–110.
- (12) Kumar, S. and Kruth, J. P. (2008), “Wear Performance of SLS/SLM Materials,” *Advanced Engineering Materials*, **10**(8), pp 750–753.
- (13) Sun, Y., Moroz, A., and Alrbaey, K. (2013), “Sliding Wear Characteristics and Corrosion Behaviour of Selective Laser Melted 316L Stainless Steel,” *Journal of Materials Engineering and Performance*, **23**(2), pp 518–526.
- (14) Zhu, Y., Zou, J., Chen, X., and Yang, H. (2016), “Tribology of Selective Laser Melting Processed Parts: Stainless Steel 316L under Lubricated Conditions,” *Wear*, **350–351**, pp 46–55.
- (15) Zhu, Y., Chen, X., Zou, J., and Yang, H. (2016), “Sliding Wear of Selective Laser Melting Processed Ti6Al4V under Boundary Lubrication Conditions,” *Wear*, **368–369**, pp 485–495.
- (16) Davim, J. P., Marques, N., and Baptista, A. M. (2001), “Effect of Carbon Fibre Reinforcement in the Frictional Behaviour of PEEK in a Water Lubricated Environment,” *Wear*, **251**(1), pp 1100–1104.
- (17) Davim, J. P. and Cardoso, R. (2009), “Effect of the Reinforcement (Carbon or Glass Fibres) on Friction and Wear Behaviour of the PEEK against Steel Surface at Long Dry Sliding,” *Wear*, **266**(7–8), pp 795–799.
- (18) Davim, J. P., Marques, N., and Baptista, A. M. (2001), “Effect of Carbon Fibre Reinforcement in the Frictional Behaviour of PEEK in a Water Lubricated Environment,” *Wear*, **251**(1), pp 1100–1104.
- (19) Jiao, S. J., Zhou, H., Yang, H. Y., Gong, G. F., Chen, J. M., and Zhou, H. D. (2003), “Tribological Behavior of Filled Polyetheretherketone Composites in Sliding against Stainless Steel under Water Lubrication,” *Mocaxue Xuebao (Tribology) (China)*, **23**, pp 385–389.
- (20) Zhang, Z. H., Nie, S. L., Yuan, S. H., and Liao, W. J. (2015), “Comparative Evaluation of Tribological Characteristics of CF/PEEK and CF/PTFE/Graphite Filled PEEK Sliding against AISI630 Steel for Seawater Hydraulic Piston Pumps/Motors,” *Tribology Transactions*, **58**(6), pp 1096–1104.
- (21) Li, D. L., Liu, Y. S., Deng, Y. P., Fang, M. S., and Wu, D. F. (2017), “The Effect of Different Temperatures on Friction and Wear Properties of CFRPEEK against AISI 431 Steel under Water Lubrication,” *Tribology Transactions*, **61**(2), pp 1–10.
- (22) Liu, Y. S., Wu, D. F., He, X. F., and Li, Z. Y. (2009), “Materials Screening of Matching Pairs in a Water Hydraulic Piston Pump,” *Industrial Lubrication & Tribology*, **61**(2–3), pp 173–178.
- (23) Dong, C. L., Yuan, C. Q., Bai, X. Q., Yang, Y., and Yan, X. P. (2015), “Study on Wear Behaviours for NBR/Stainless Steel under Sand Water-Lubricated Conditions,” *Wear*, **332–333**, pp 1012–1020.
- (24) Wu, D. F., Liu, Y. S., Yang, S. D., Yang, Z., and Tang, H. (2012), “Friction and Wear Characteristics of WC-10Co-4Cr/Si₃N₄ Tribopair Lubricated under Silt-Laden Water,” *Wear*, **294–295**, pp 370–379.
- (25) Davim, J. P. and Marques, N. (2001), “Evaluation of Tribological Behaviour of Polymeric Materials for Hip Prostheses Application,” *Tribology Letters*, **11**(2), 91–94.
- (26) Zhu, Y., Lin, G. L., Khonsari, M. M., Zhang, J. H., and Yang, H. Y. (2018), “Material Characterization and Lubricating Behaviors of Porous Stainless Steel Fabricated by Selective Laser Melting,” *Journal of Materials Processing Technology*, **262**, pp 41–52.